Hindawi
Shock and Vibration
Volume 2019, Article ID 3742512, 14 pages
https://doi.org/10.1155/2019/3742512

*Research Article*

# Research on Rolling Bearing Fault Feature Extraction Based on Singular Value Decomposition considering the Singular Component Accumulative Effect and Teager Energy Operator

**Longlong Li, Yahui Cui, Runlin Chen, Lingping Chen, and Lihua Wang**

*School of Mechanical and Precision Instrument Engineering, Xi'an University of Technology, Xi'an, China*

Correspondence should be addressed to Yahui Cui; cyhxut@xaut.edu.cn

Received 7 April 2019; Revised 17 September 2019; Accepted 9 October 2019; Published 30 October 2019

Academic Editor: Paola Forte



The extraction of impulsive signatures from a vibration signal is vital for fault diagnosis of rolling element bearings, which are always whelmed by noise, especially in the early stage of defect development. Aiming at the weak defect diagnosis, kurtosis of Teager energy operator (KTEO) spectrum is employed to indicate the fault information capacity of a spectrum, and considering the accumulative effect of a singular component, accumulative kurtosis of TEO (AKTEO) is firstly proposed to determine the proper signal reconstructed order during vibration signal processing using singular value decomposition (SVD). Then, a vibration processing scheme named SVD-AKTEO is designed where an iteration is employed to reflect an accumulative singular effect by kurtosis of TEO spectrum. Finally, the fault diagnosis results can be extracted from the TEO spectrum output by SVD-AKTEO. Simulation data and real data from a run-to-failure experiment of a rolling bearing are adopted to validate the efficiency, and comparative analysis demonstrates the feasibility to detect the early defect of the rolling bearing.

## 1. Introduction

Rotating machinery is extensively used in modern industry, and its critical components of the machine, rolling element bearings (REBs), are easily prone to failure due to heavy load, long-term, and severe operation environment. Therefore, condition monitoring and fault diagnosis have been a research shot in recent years. As an essential part to support rotating components in most rotating machines, the rolling bearing plays a crucial role in the functioning and overall performance of machinery [1, 2]. All kinds of REB have wide applications due to their relatively lower price and easy installation. However, even a little malfunction of REB may result in unexpected breakdown or shutdown, and they account for equipment failures to almost 45–55% [3]. Therefore, the fault diagnosis of REB, especially in the early period of defects, is under high demand to ensure the safe operation of rotating machinery and prevents both equipment accidents and maintenance costs.

There are various condition-related monitoring information such as acoustic emission (AE) [4], oil debris analysis [5], motor current signature analysis [6], vibration signal [7], and so on, and vibration signal-based techniques are preferred due to low cost and easy installation of an accelerometer. In addition, the vibration signal has been proven accurate enough to capture fault signatures of REB, and some efficient signal processing schemes based on vibration signal for bearing fault diagnosis has been developed recent years [8]. A new bearing fault diagnosis approach based on vibration signal is proposed by integrating the fine-to-coarse multiscale permutation entropy, Laplacian score, and support vector machine, and the entropy-based features are extracted from the bearing vibration signal [9]. Spall is a common defect of bearing, and a technique is proposed, which estimates the spall size by detecting the entry point by variational mode decomposition (VMD) and the exit point by differentiation technique [10]. Among the main steps of fault diagnosis,

feature extraction is critical for fault diagnosis and always relies on signal processing techniques, and it is crucial to select an appropriate method to process the vibration signal. Therefore, kinds of signal processing techniques have been developed in recent years, and they are reviewed in detail by Akhand and S. H. [8].

SVD is a traditional signal processing applied in speech recognition, signal purification, and feature extraction, and it has drawn increasing attention in rotating machinery fault diagnosis. The main fault diagnostic approaches based on SVD can be assorted into three categories. Firstly, some indexes are proposed based on the singular values (SVs). Cong et al. introduced the singular value ratio (SVR) to the SVD-based vibration signal processing and proved that the SVR had a good local identification capability to extract fault features [11]. Zhao et al. proposed the concept of difference spectrum of a singular value, which was specifically the forward difference of a singular value sequence to capture the sudden change status of singular values of a complicated signal [12]. Secondly, some statistics indexes are employed to select singular components obtained from Hankel matrix-based SVD and kurtosis is one of them, which was applied as a criterion to select fault SCs whose kurtosis values were greater than 3. By summing up the selected SCs, the weak fault is extracted clearly in both artificial simulation and actual experimental data [13]. However, the SVs mainly reflect the energy of the decomposed SCs, which may ignore the weak fault caused by an incipient defect. Aiming at solving this problem, other fault indexes calculated on SC are put forward, which is the third category of SVD-based defect diagnosis. A reweighted SVD is put forward based on a novel information index named periodic modulation intensity (PMI), which was calculated on each SC, and the SCs with PMI value larger than 1 are chosen to form the denoised SC, from that the early fault can be extracted successfully [14]. In addition, the SVs or features extracted from SCs or combination from both of them can be regarded as feature vectors fed into convolutional neural network (CNN), support vector machine (SVM), and other pattern recognition techniques for fault type identification. According to the decomposition principle of SVD, a vibration signal can be reshaped into various types of Hankel matrix which are decided by the matrix order, and the contribution of defect unrelated components such as background noise is almost equally decomposed into each SC; in order words, the fault-sensitive component and the insensitive ones are almost evenly distributed in each SC, resulting in deficiency in SVD signal processing. Therefore, some new indexes are under high demand to efficiently extract the fault-induced or sensitive component to the most extent.

Considering the singular component accumulative effect, the accumulative component kurtosis (ACK) is proposed to find out the fault-sensitive singular component during an iteration where each single SC is added to the accumulative one [15]. Since fault characteristic frequency is obtained by the frequency domain of the vibration signal, the ACK is not a very ideal index to choose fault-sensitive singular component due to that the ACK is the kurtosis value of the waveform of accumulative singular component, which is a statistical indicator not a fault index. Since the fault diagnosis results are always derived from the envelope spectrums, indexes from the frequency domain may more directly reflect the quantity of defect information. Towards to finding a more direct parameter, the kurtosis of the squared envelope spectrum (SES) is later employed to assist the SVD to select the defect-related singular component and based on that, the SVD-KSES scheme was put forward to extract the early fault features of the rolling bearing [16]. As an alternative signal demodulation method, the Teager energy operator enhances the signal transient characteristics and is sensitive to the shock components of a signal, which improves the signal-to-noise ratio (SNR) and makes the impulse fault features more reliable [17]. Moreover, the TEO is also a nonlinear energy tracking operator using simple mathematical method to analyze and track the signal energy which also avoids the occurrence of negative frequency [18]. Consequently, the TEO is applied here as a good substitute of Hilbert transform-based signal demodulation to assist SVD for bearing fault signal processing.

The vibration signal of malfunctioned rolling bearing under operation presents lots of impulses due to the collisions between defective area and its mating surface. Kurtosis is a statistic indictor extensively used to measure the signal impulsiveness and also a dimensionless parameter that is sensitive to impact signals. However, the random impacts, heavy background noise, and rolling element slip make the impulses not equally spaced in time domain, thus leading to kurtosis inefficiency in the fault diagnosis [19]. Since to extract fault characteristic frequency (FCF) in the envelope spectrum is practical and widely used in fault diagnosis of REB and TEO spectrum's superiority over HT-based envelope analysis, the TEO spectrum amplitude can provide easy recognition of FCF, and the fault frequency lines are equally separated in the spectrum. The larger the amplitude of the FCF lines is, the more serious the fault is. Consequently, motivated by the Protrugram [20] proposed by Barszcz et al., the kurtosis of the frequency domain could be used as a measuring indicator of the defective information, and then the kurtosis of TEO spectrum amplitude (KTEO) is employed here to choose defect-sensitive SC from the view of the frequency domain.

Based on the above introduction, considering the accumulative singular component effect during the SVD signal processing and the superiority of TEO, a fault diagnosis scheme named SVD-AKTEO is proposed. In the SVD-AKTEO, the collected vibration signal is firstly fed to the Hankel-based SVD to obtain a set of SCs, and after that, the accumulative singular component (ASC) is set during an iteration where each singular component is added to the ASC one by one. Afterwards, the TEO spectrum of ASC is calculated once a new SC is added to ASC. Finally, from the variation of TEO amplitude kurtosis, the fault-sensitive SCs can be identified, and their sum can be taken as the fault characteristic component; from its TEO spectrum, the fault diagnosis can be finally obtained. The practicability of SVD-AKTEO is validated by an artificially simulated signal of a REB with bearing defective outer raceway, and its performance is comparatively analyzed with SVD-ACK and SVD-

KSES. Subsequently, a public dataset from a run-to-failure experiment is introduced to verify the feasibility of SVD-AKTEO; both the simulation and experimental results illustrate the SVD-AKTEO has some superiority over the two primary methods to extract defective information, especially the fault in an early stage.

The rest of this paper is arranged as follows. Section 2 reviews Hankel matrix-based SVD and TEO, respectively. In Section 3, the performance of KTEO is evaluated, as well as its superiority over the waveform kurtosis. Subsequently, the SVD-AKTEO is proposed and illustrated in detail. Then, the simulation of a REB with defective outer raceway is conducted to verify the SVD-AKTEO by contrastive analysis with the two previously proposed methods in Section 4, and Section 5 verifies the SVD-AKTEO with the actual experimental data from NSF I/UCR Center for Intelligent Maintenance Systems (IMS). Finally, the conclusions are drawn in Section 6.

## 2. Theoretical Background

*2.1. Hankel Matrix-Based Singular Value Decomposition.* SVD is a conventional matrix decomposition method which can decompose any real matrix $M \in R_{m\times n}$ into three matrices: the left orthogonal matrix $U \in R_{m\times n}$, the diagonal matrix $D \in R_{m\times n}$, and the right orthogonal matrix $V \in R_{m\times n}$:

$$M = UDV^T, \tag{1}$$

where $D = (\text{diag}\ (\sigma_1, \sigma_2, \sigma_3, \ldots, \sigma_L), O)$, $L = \min\ (m, n)$, and $\sigma_1 > \sigma_2 > \sigma_3, \ldots > \sigma_L$. $\sigma_i$ $(i = 1, 2, \ldots, L)$ are the singular values of the matrix $M$ and listed by descending order by their value.

The acquired vibration signal is always collected in time series on which SVD cannot implement directly, and Hankel matrix is most extensively applied one among the various matrix formats such as Toeplitz matrix, cycle matrix, and Hankel matrix [21] Here, the collected original vibration signal is assumed to be $x = (x(1), x(2), \ldots, x(N))$, and according to the phase space reconstruction theory, a Hankel matrix $X$ can be reshaped from signal $x$ as follows:

$$X = \begin{bmatrix} x(1) & x(2) & \cdots & x(n) \\ x(2) & x(3) & \cdots & x(n+1) \\ \cdots & \cdots & \ddots & \cdots \\ x(N-n+1) & x(N-n+2) & \cdots & x(N) \end{bmatrix}, \tag{2}$$

where $1 < n < N$ and $m = N - n + 1$; then, $X \in R_{m\times n}$ represents the reconstruction of the attractor orbit matrix. Since this matrix is reconstructed by the collected vibration signal with background noise, $X$ can be expressed as $X = D + W$, where $D$ represents the $(N - n + 1) \times n$ matrix of the smooth signal in the reconstruction space while $W$ represents the $(N - n + 1) \times n$ matrix of the noise interference signal. Applying equation (1) in equation (2), the trajectory matrix $X$ can be decomposed into three matrixes according to the SVD principle:

$$X = UDV^T, \tag{3}$$

$$U = [u_1, u_2, \ldots, u_n], \tag{4}$$

$$V = [v_1, v_2, \ldots, v_n], \tag{5}$$

$$D = \begin{bmatrix} \sigma_1 & & & 0 \\ & \sigma_2 & & \\ & & \ddots & \\ 0 & & & 0 \end{bmatrix}, \tag{6}$$

where $U$ represents the left singular matrix and $V$ represents the right one; the value of the diagonal of matrix $D$ is composed of the singular values list with the descending order. $u_i$ is the $i$th column vector of the singular $U$, and $v_i$ is the $i$th column vector of singular matrix $V$. Therefore, $X$ can be summed up as

$$X = \sigma_1 u_1 v_1 + \sigma_2 u_2 v_2 + \cdots + \sigma_m u_m v_m. \tag{7}$$

Finally, a new Hankel matrix $X'$ can be obtained by removing the noise components and defect unrelated component via setting the singular values corresponding to the noise components and interference of random impulses to 0. After removing the noise and the fault unrelated component, the time series of vibration signal should be extracted from the matrix one by Hankel principle, and their two simple approaches can be employed for this purpose. One is the reverse Hankel reconstruction shown in Figure 1(a) while the second one is the antidiagonal element averaging technique shown in Figure 1(b), and its calculating equation is presented as

$$x_i = \frac{1}{\beta - \alpha + 1} \sum_{j=\alpha}^{\beta} X'_{i-j+1,j}. \tag{8}$$

*2.2. Teager Energy Operator.* The Teager energy operator is originally proposed for nonlinear speech processing and latterly introduced into the field of fault diagnosis [22]. Hilbert transform-based envelope analysis processes the acquired vibration signal into an analytical signal by HT, while TEO can be implemented directly on the signal by using a simple mathematical method. For any signal $x(t)$, its TEO denoted by $\psi(\cdot)$ can be defined as equation (9) in its continuous case and discrete one is shown in (10), respectively:

$$\psi[x(t)] = \left(\frac{dx(t)}{dt}\right)^2 - x(t)\frac{d^2x(t)}{dt^2} = [\dot{x}(t)]^2 - x(t)\ddot{x}(t), \tag{9}$$

$$\psi[x(n)] = x^2[n] - x[n-1]x[n+1]. \tag{10}$$

The output of the TEO is a product of the instantaneous amplitude of a vibration signal and the square of the instantaneous frequency, which is reported to have a good potential of tracking the instantaneous energy of the signal,

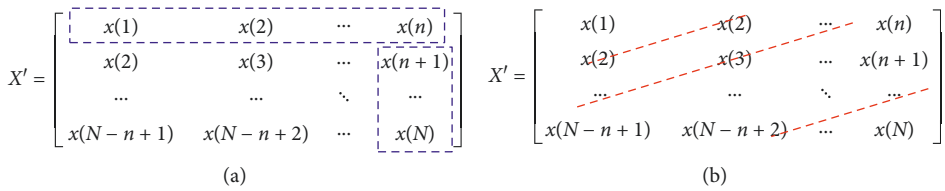


Figure 1: Two approaches to convert Hankel matrix signal to time series one.

and this quality is supposed to be effective to enhance the impulsive features of the vibration signal [23].

## 3. SVD-AKTEO Method

The vibration signal of a defective rolling bearing not only presents a series of impulses in the waveform but also an equal-spaced frequency lines in the envelope spectrum and TEO spectrum. Thus, the fault signal can be simulated by a numerical method with the parameters mentioned in Reference [16]. The waveforms in Figure 2(a) are the artificial defect-induced periodic impulses in the vibration signal and the noisy one with SNR −12, respectively. Then, the series of nearly equal time interval impulses are employed here to evaluate defect-indexing performance of the kurtosis of TEO. Figure 2 shows several TEO spectrums by applying with different noisy signals to the periodic impulses. The SNR varies from −12 to 10, but only three TEO spectrums with SNR −8, −10, and −12 are plotted in Figures 2(b)–2(d), respectively, from which it can be inferred that the FCF lines are clearer to be observed when the SNR gets higher. In other words, the more noise will blur the FCF, thus providing little fault information about the fault recognition. In addition, the waveform kurtosis along with the KTEO with the SNR ranging from −12 to 10 are plotted in Figure 3. From the overview, the two parameters grow up when the noise SNR gets higher, but three distinctive range can be partitioned and labelled by ranges A, B, and C. The A range donates the heavy noise during which the two indexes have no obvious increase while the C range witnesses an interesting trend that the KTEO varies little, but the kurtosis of waveform grows up when the SNR improves. However, range C locates in a very high SNR that there is no necessity to decompose the signal to improved signal quality. In range B, the KTEO grows sharp that kurtosis when the noise SNR varies from −10 to 0, that is to say, the KTEO has better fault identifying performance than kurtosis. Therefore, the KTEO is employed here as an index to find out the fault-sensitive singular components.

On the basis of the analysis above, the accumulative singular component KTEO (AKTEO), as a fault information-measuring parameter, is proposed to select the defect-sensitive SC during the process of Hankel matrix-based SVD, and a fault diagnosis scheme name SVD-AKTEO is proposed to extract fault feature automatically. The procedure of SVD-AKTEO is presented in Figure 4, and the detailed process is as follows:

(1) The vibration signal is collected by the accelerometer installed in the bearing housing.

(2) The raw vibration signals are reshaped into Hankel matrixes and following that, the SVD and reverse Hankel construction are implemented to decompose the raw signal into several SCs listed by descending order of their SV values.

(3) Let the ASC equals the first SC, then calculate the TEO spectrum of an accumulative singular component (ASC), as well as the KTEO value. After that, the TEO spectrum and the KTEO value should be obtained once a new SC is added into the ASC. During this process, the KTEO can indicate the influence of each single SC to the final accumulative SC, which is expected to find out the appropriate order to decide the fault-sensitive SC, and removing the noise component or defect unrelated SC.

(4) Extract the fault characteristics from the TEO spectrum and defect identification by comparing with the theoretical frequency lines.

## 4. Numerical Simulation Analysis

*4.1. The Simulated Signal.* To verify the proposed SVD-AKTEO method, an artificial fault signal of rolling bearing is analyzed in this section. The simulated signal is modelled as a series of damping oscillation waveforms and reported as an amplitude-modulated signal in which the fault characteristic frequency is modulated to a high resonance frequency carrier. For numerical simulation, the vibration signal collected by the accelerometer can be regarded as a series of impulses, and each impulse with exponential attenuation can reflect the vibration response of signal travelling path influence. Therefore, the simulated fault vibration signal of outer race defect can be defined as follows:

$$\begin{cases} x(t) = \sum_{i=1}^{M} A_i s(t - iT) + n(t), \\ s(t) = e^{-\beta t} \cos(2\pi f_r t), \end{cases} \tag{11}$$

where $A_i$ is the $i$th shock impulse's amplitude, $T$ represents the time period which is in accordance with the characteristic frequency, and $n(t)$ represents the Gauss white noise. $M$ is the number of impulses. $s(t)$ is defined as a damping oscillation waveform, $\beta$ is the damping coefficient, and $f_r$ denotes the modulation frequency, which simulates the resonance information of the system [24]. $T$ equals 1/105.5 = 0.0095 s, and sampling time is 0.2 s; the other parameters are listed in Table 1. The waveform of the simulated signal is plotted in Figure 5 by a red line and the noisy signal with SNR −13 by the blue color. The envelope

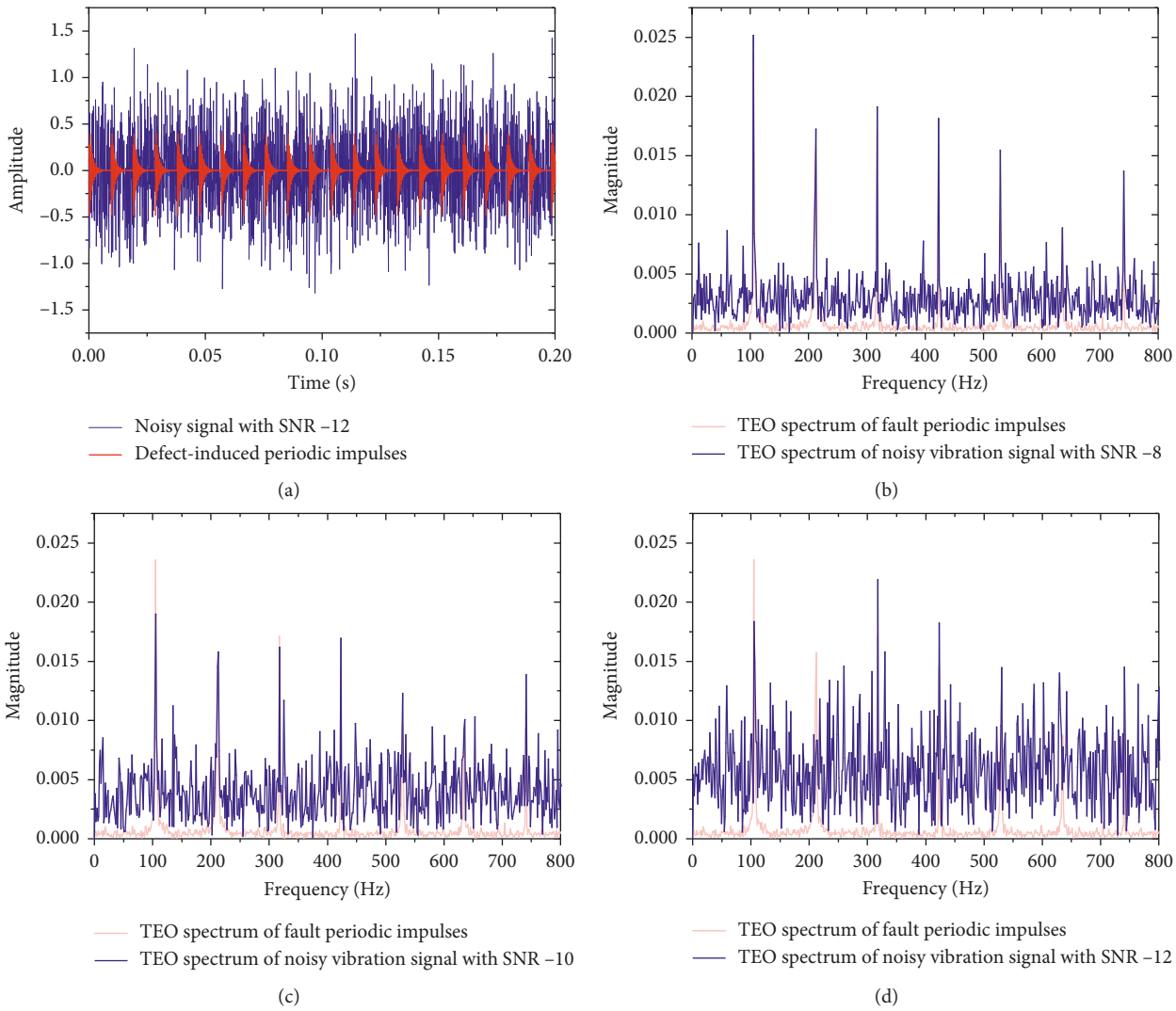


Figure 2: TEO spectrums with different SNRs. The input signal (a) SNR −6, (b) SNR −8, (c) SNR −10, and (d) SNR −12.

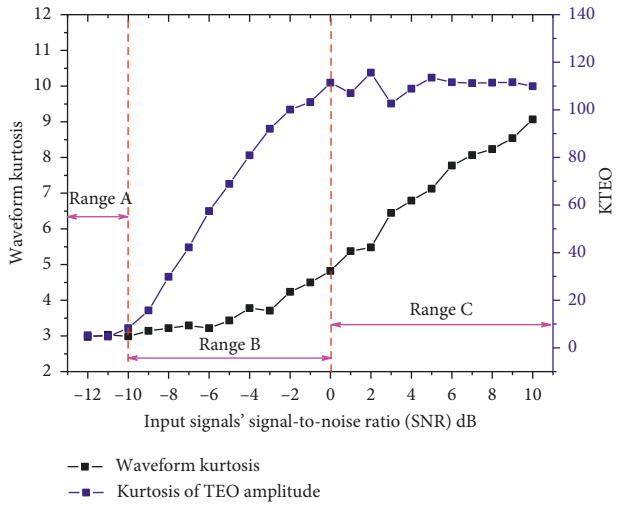


Figure 3: Waveform kurtosis and kurtosis of TEO amplitude variation with signal-to-noise ratio.

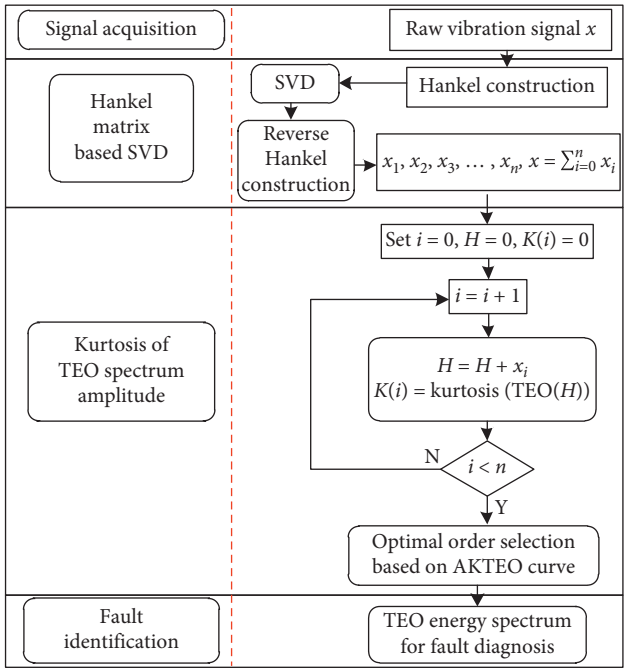


Figure 4: The framework of SVD-KTEO.

Table 1: Parameter for REB fault signal simulation with outer raceway defect.

| Impulse amplitude | Rotating speed | Natural frequency | Fault frequency | Sampling frequency |
|---|---|---|---|---|
| 0.5 | 1772 rpm | 2000 (Hz) | 105.5 (Hz) | 12000 (Hz) |

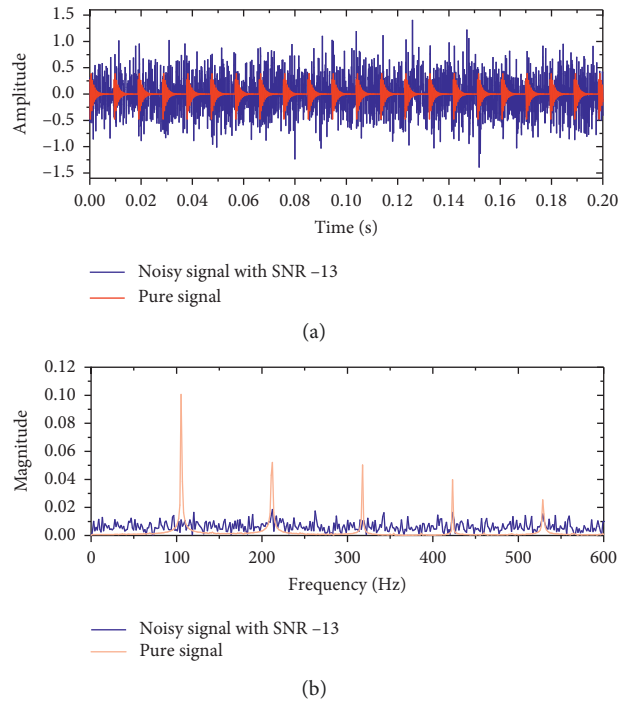


Figure 5: Simulated vibration signals of outer race fault with and without noise signal and their envelope spectrums. (a) Waveforms of the both signals. (b) Envelope spectrum of the two signals.

spectrum of the noise-contaminated signal is shown in Figure 5(b) along with the pure signal' envelope spectrum as a reference. It is clear that there are no evident frequency peaks sticking out at the FCF line due to the presence of heavy background noise.

*4.2. The Contrastive Analysis of the Proposed Method.* In order to evaluate the fault feature extraction performance of the proposed method SVD-AKTEO, the noisy signal with SNR −13 denoted by the blue line in Figure 5(a) is fed to SVD-AKTEO, and the SC number is set to 15. Accordingly, there are 15 SCs, and these SCs undergo the third step of the procedure: the iteration of ASC. Each TEO spectrum of the ASC can be obtained as well as the kurtosis values of TEO spectrum, depicted in Figure 6. The highest kurtosis appears when the former two SCs are added together. Therefore, according to the principle of SVD-AKTEO, the sum of the two SCs is regarded as the output result, shown in Figure 7. Apparently, some impact components can be observed from the waveform of the SVD-KTEO output, and the TEO spectrum shows the domain characteristic frequency 105.5 Hz and its harmonics, which preliminarily demonstrates the outer ring defect has happened in the rolling bearings as a result of the characteristic frequency being very close to the outer raceway defect frequency BPFO. Furthermore, the comparison of Figures 7 and 5 verifies that the SVD-AKTEO can effectively extract the fault features for bearing fault diagnosis.

Since SVD-AKTEO is enhanced on the SVD-KSES and SVD-ACK, the comparative analysis of the third one could be interesting. Then, the signal shown in Figure 5 is also fed to other two approaches, respectively. The kurtosis of SES variation is plotted in Figure 8, from which and according to the principle of SVD-KSES, the first singular component can be taken as the output result which is shown in Figure 9. The fault-induced periodic impacts are more obvious, and evident characteristic frequency can be easily observed in its envelope spectrum, as well as its harmonics. Similarly, the accumulative component kurtosis is plotted in Figure 10, and the waveform of SVD-ACK output is shown in Figure 11(a) and the envelope spectrum in Figure 11(b). In spite of the prominent characteristic frequency and its harmonics emerging in Figures 7(b), 9(b), and 11(b), respectively, it should be noticed that they are plotted with different $y$ scales and straightforwardly, they are plotted in one figure with the same dimensions, shown in Figure 12. Undoubtedly, the characteristic frequency lines of the SVD-AKTEO is the lowest one when compared with the other two approaches, while higher frequency lines companied by higher noise can be observed from the spectrum lines denoted by the black and blue colour in Figure 12. However, the TEO spectrum of SVD-AKTEO output provides the equivalent fault diagnosis performance by clearly presenting the characteristic frequency and its harmonics with the lowest signal energy; from another point of view, SVD-AKTEO has a better defect feature extraction performance from low energy signal.

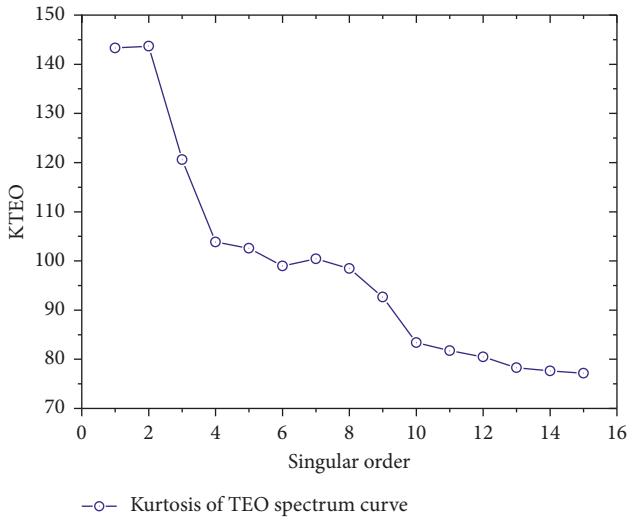


Figure 6: Kurtosis of TEO spectrum variation with singular order.

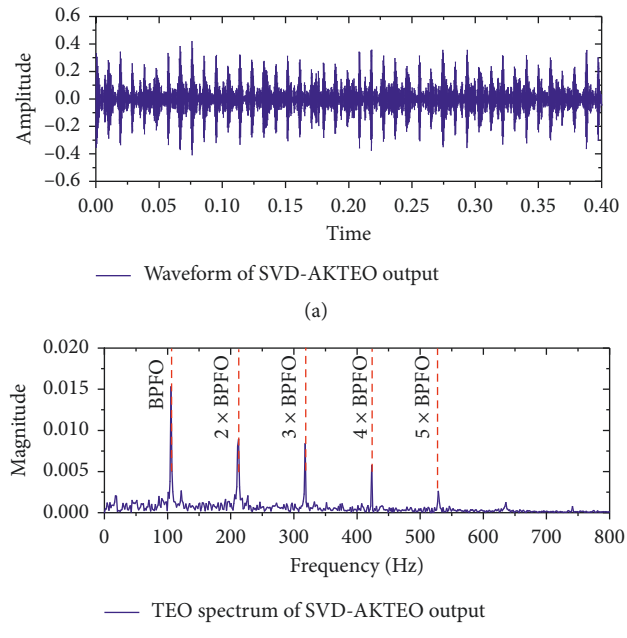


Figure 7: Output of SVD-AKTEO. (a) The waveform of SVD-AKTEO output. (b) The TEO spectrum of the signal in (a).

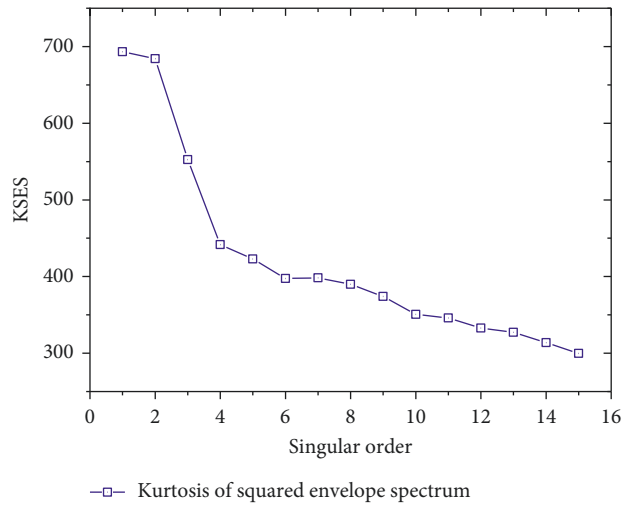


Figure 8: Kurtosis of the squared envelope spectrum variation with singular order.

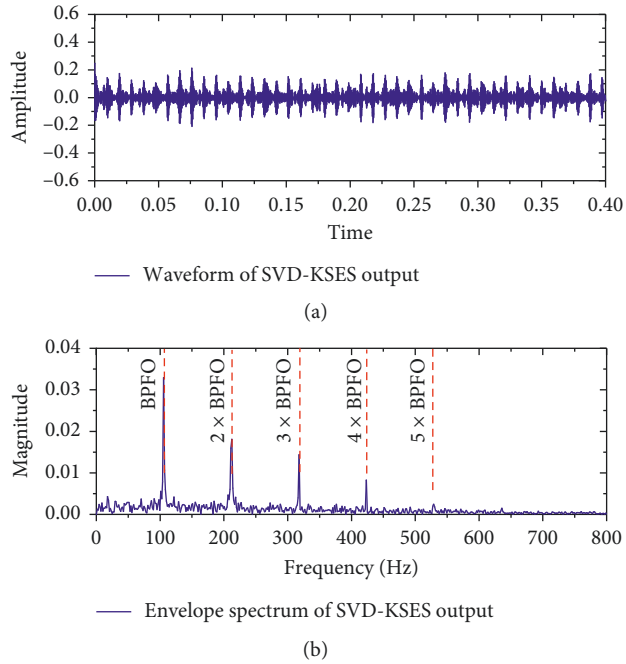


Figure 9: Output of SVD-KSES. (a) The waveform of SVD-KSES output. (b) The envelope spectrum of the signal in a.

## 5. Experimental Validation

*5.1. Experiment Layout and Description.* To further verify the proposed SVD-AKTEO scheme, the experimental data provided publicly by NSF I/UCRC for Intelligent Maintenance System (IMS) [25] are adopted in this section. As shown in Figure 13(a), there were four bearings with the same type ZA-2115 installed on a shaft driven by an AC motor via rub belts, and the rotating speed was kept at 2000 rpm constantly. The structural parameters of the tested bearing are listed in Table 2. A radial load of 6000 lbs was applied on the bearing 2 and 3. Two ICP accelerometers, as depicted in Figure 13(b), were equipped on each bearing house and collected vibration signals from $x$ and $y$ directions with a National Instruments DAQ Card-6062E at sampling rate 20 kHz [16]. In addition, the four bearings were force lubricated, and a magnet was planted to gather the wearing or fault-induced debris in the oil circulation. The test would be switched down automatically if the amount of the adhered debris or bearing temperature reached a preset level. No. 2 dataset is used to verify the proposed method in this section. Each data file of the 984 sets was collected every 10 min and contains 20,480 data points. At the end of the experiment, wear-out failure occurred on the outer ring, and the run-to-failure data had

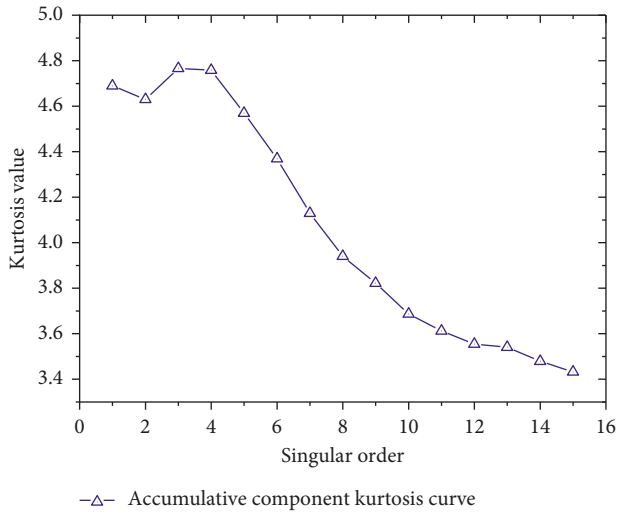


Figure 10: Kurtosis of accumulative singular component variation with singular order.

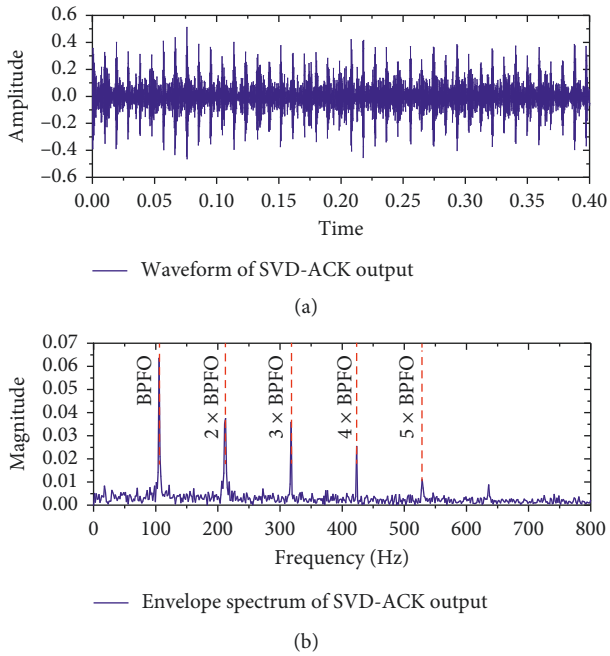


Figure 11: Output of SVD-ACK. (a) The waveform of SVD-ACK output. (b) The envelope spectrum of the signal in a.

been acquired. The fault frequency of the outer ring defect can be computed according to the equation and arguments in Table 3.

*5.2. Experimental Validation and Contrastive Analysis.* Since root mean square (RMS) is not only a commonly used statistical parameter to quantify the collected bearing run-to-failure vibration signals [26] but also a general evaluation indicator of a system. Therefore, the RMS variations over the service life of bearing 1 with experimental condition 2 are plotted in Figure 14, and for a convincing illustration, the reference threshold is empirically set based on the first two

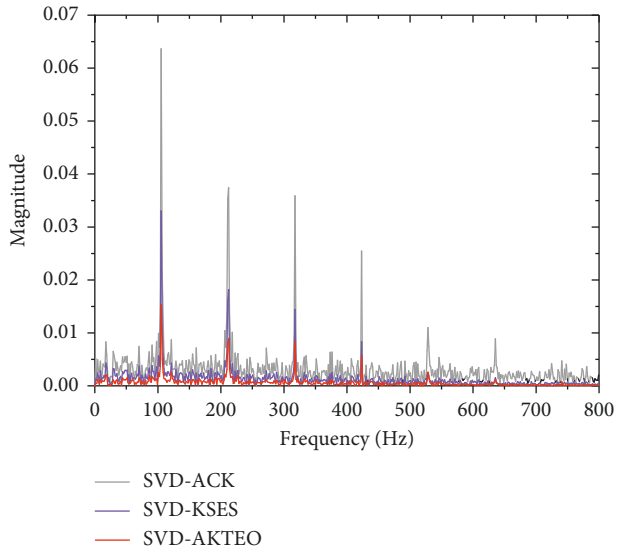


Figure 12: Frequency domain contrastive analysis of the outputs of three methods: SVD-ACK, SVD-KSES, and SVD-AKTEO.

hundred datasets and dotted by the red colour; the threshold value equals the mean plus three times the standard deviation (i.e., threshold $= \mu + 3\sigma$) [27]. It is clear that, after the long term of normal operation, the bearing steps into an abnormal running stage, indicating some defects occurring on the bearing. In addition, to make things clearer, two specific dataset number labelled A and B are selected, and the envelope spectrums of the selected vibration signals are shown in Figure 15, as well as the waveforms in Figures 15(a) and 15(c), respectively.

From the envelope spectrum depicted in Figure 15(b), it can be confirmed that the bearing undergoes the outer ring defect by the evident FCF lines. However, the waveform of signal at time B, presented in Figure 15(c) is not so impulsive as the one in Figure 15(a), and its envelope spectrum in Figure 15(d) also fails to determine the fault type. Consequently, the signal plotted in Figure 15(c) with relative heavy noise should be fed to SVD-AKTEO for extracting some more fault information.

To verify the SVD-AKTEO, the early faulty signal of bearing 1 shown in Figure 15(c) undergoes the procedure described in Figure 4, and the singular order is set to 8. Then, the kurtosis of TEO spectrum curve is obtained as shown in Figure 16. According to the principle of SVD-AKTEO, the first accumulative SC should be regarded as the output result, and its waveform is presented in Figure 17(a) and the TEO spectrum of the signal in Figure 17(b). The waveform presents clearly impulsive, which predicts some incipient defect occurring internal of bearing 1, and from the TEO spectrum in Figure 17(b), it can be easily confirmed that there is the outer ring defect by the outer raceway fault characteristic frequency and its three times frequency lines.

To better demonstrate the SVD-AKTEO's superiority over the other two methods, the signal of dataset 535 also experiences the procedure of SVD-ACK and SVD-KSES. The ACK curve is plotted in Figure 18; then, the first two SC is selected as the output of SVD-ACK according to the basic

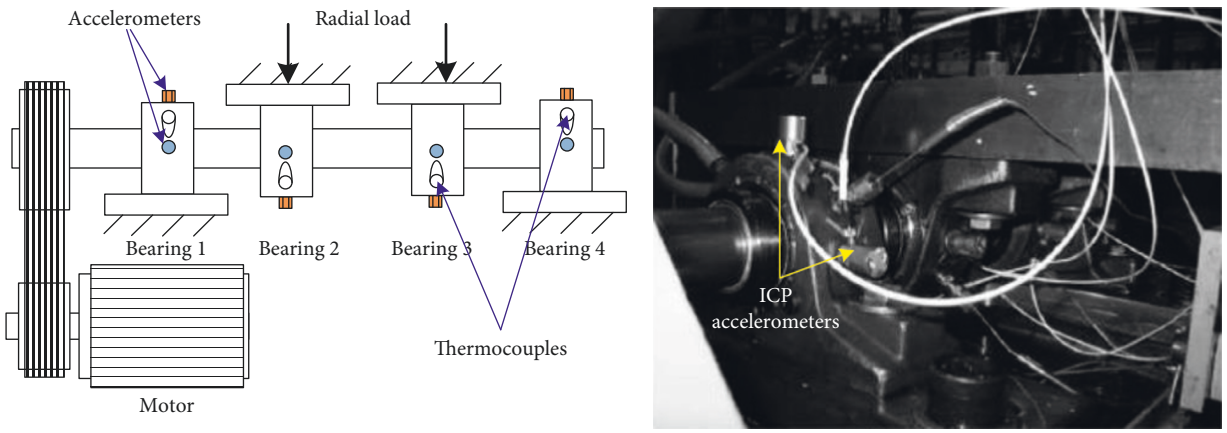


Figure 13: Schematic diagram of the experiment (a) and bearing test rig (b).

Table 2: Structural parameters of a faulty rolling bearing.

| Parameters of Rexnord ZA-2115 rolling bearing | | | |
|---|---|---|---|
| Rolling element number $n_r$ | Contact angle $\alpha$ | Ball diameter $d_r$ | Pitch diameter $D_w$ |
| 16 | 15.17° | 8.4 mm | 71.5 mm |

Table 3: Fault characteristic frequency calculation of rolling bearing Rexnord ZA-2115.

| Fault type | Fault characteristic calculation | Rotating speed | Sampling frequency | Fault characteristic frequency |
|---|---|---|---|---|
| Outer raceway | BPFO = $1/2 f_s (1 - d_r/D_w \cos\alpha) n_r$ | 2000 rpm | 20 kHz | 236.4 Hz |

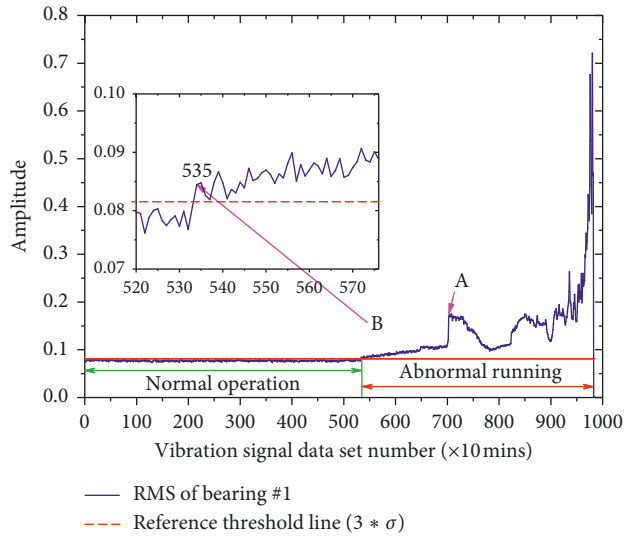


Figure 14: Vibration accelerations of bearing 1 during its run-to-failure life.

principle. Similarly, from the KSES curves in Figure 19, the first SC is taken as the output of SVD-KSES. The comparison of both approaches is presented in Figure 20; the waveform in Figure 20(a) and envelope spectrum in Figure 20(b) are for SVD-ACK, while the waveform in Figure 20(c) and envelope spectrum in Figure 20(d) are for SVD-KSES.

The waveform output by SVD-KSES is more impulsive than the one by SVD-ACK; while both of them clearly present the outer raceway characteristic frequency and its two times harmonics, the amplitudes of characteristic frequency lines in the envelope spectrum of SVD-ACK are higher than the one in Figure 20(d) by SVD-KSES since the

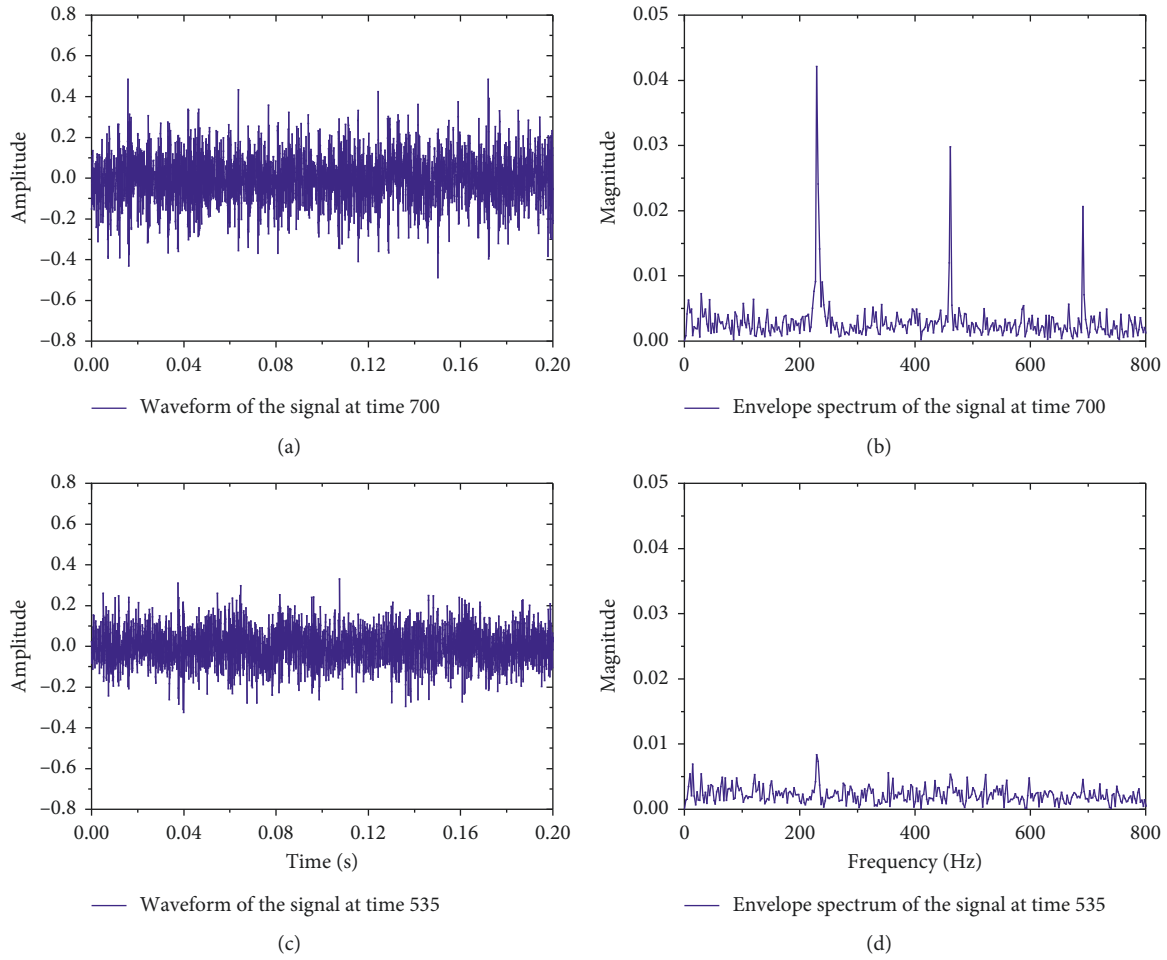


Figure 15: Waveforms of time point label A and B and their corresponding envelope spectrums. (a) and (c) represent waveforms of signals corresponding to the time point B, and (b) and (d) represent the envelope spectrums of the signal at the time point B, respectively.

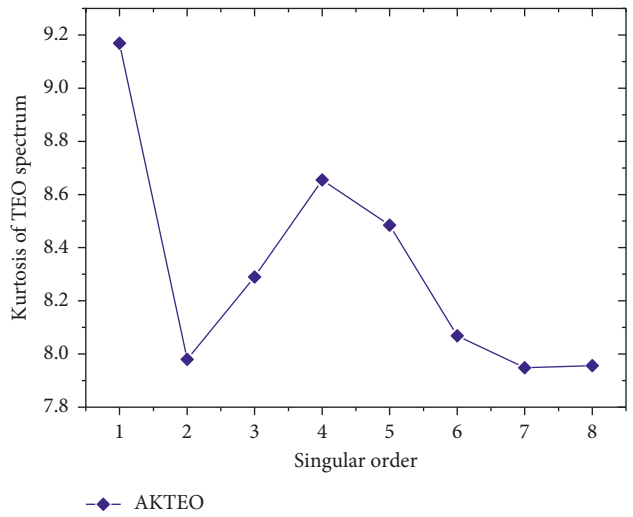


Figure 16: Kurtosis of TEO spectrum variation with singular order.

SVD-ACK chooses the first two SC as its output while the SVD-KSES just selects the first one. From Figures 17(b), 20(b), and 20(d), it can be concluded that though the SVD-KSES and SVD-AKTEO regard the first SC as the output, the later one presents the rather clear fault characteristic frequency lines with a very low energy signal, which proves the effectiveness of the proposed SVD-AKTEO to detect the early fault of rolling bearing once again.

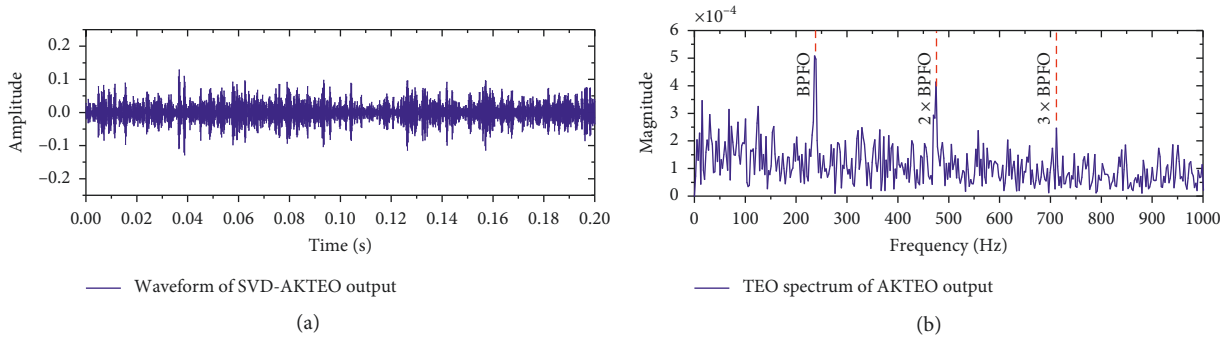


Figure 17: Output of SVD-AKTEO. (a) Waveform of the SVD-AKTEO output. (b) The TEO spectrum of the signal output by SVD-AKTEO.

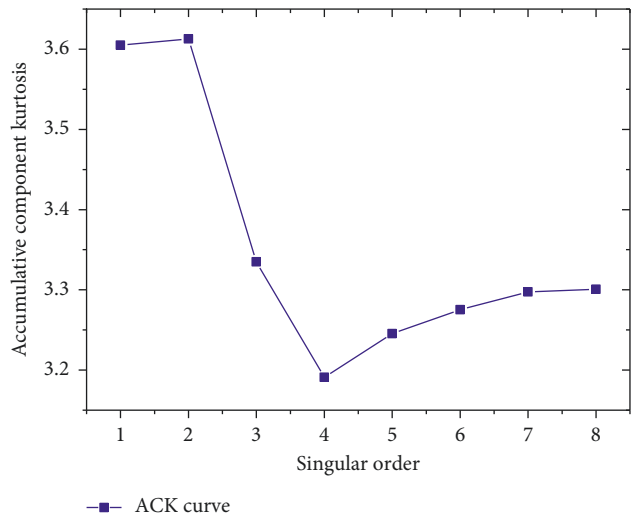


Figure 18: Accumulative component Kurtosis variation with singular order.

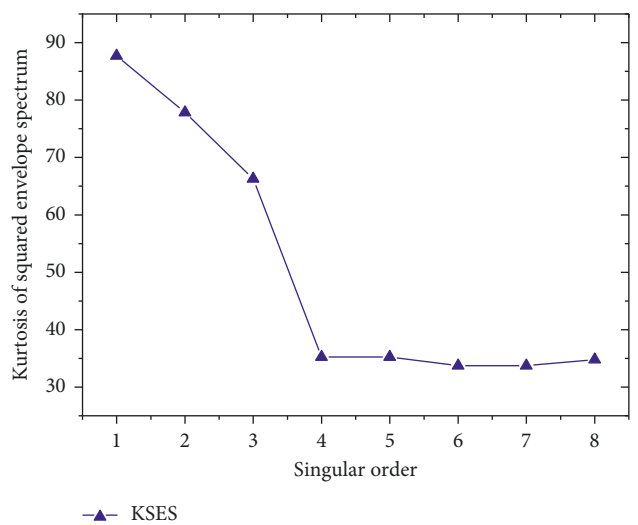


Figure 19: Kurtosis of the squared envelope spectrum variation with singular order.

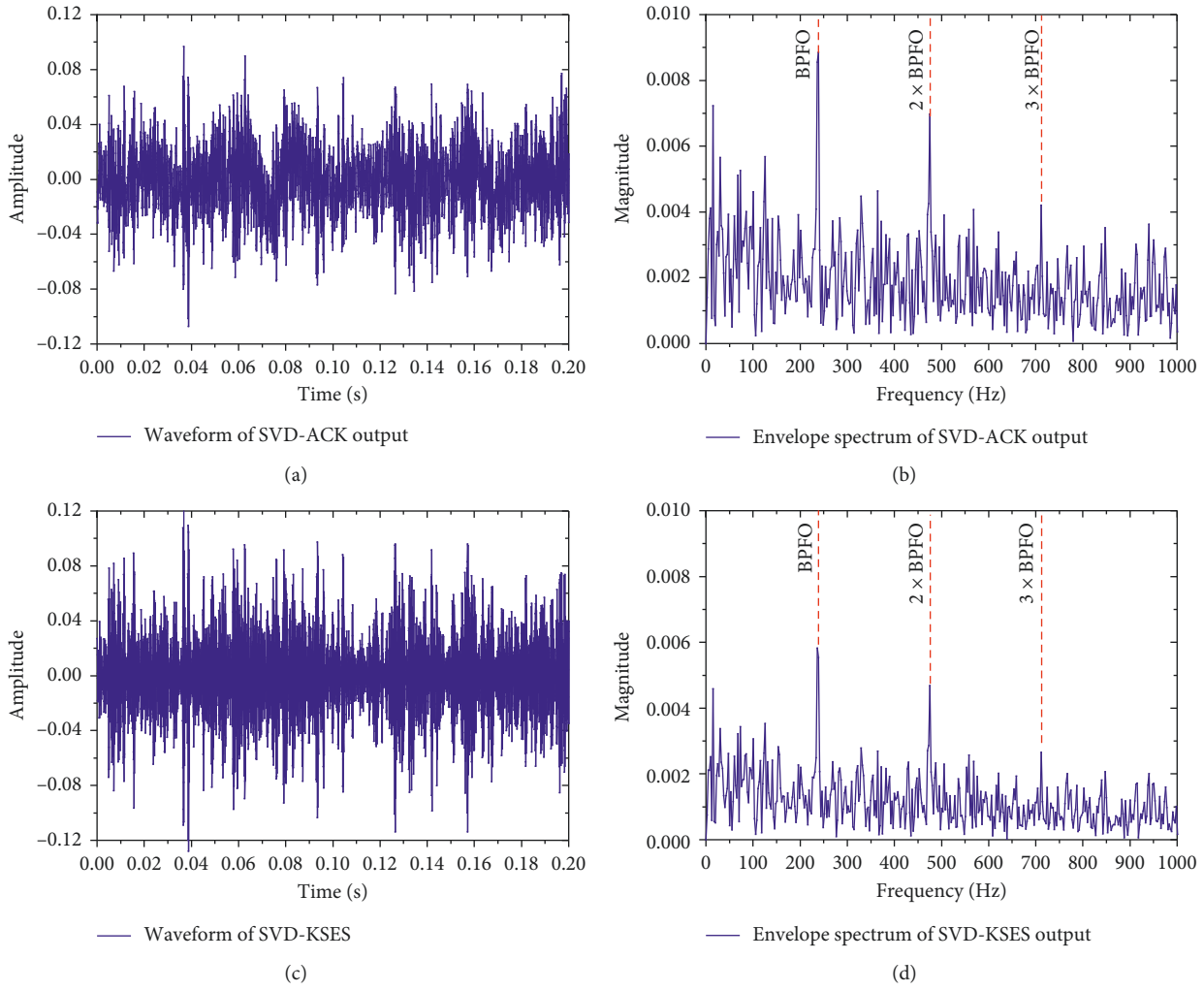


Figure 20: Comparison of experiments on SVD-ACK and SVD-KSES. (a) The waveform of SVD-ACK output. (b) The envelope spectrum of SVD-ACK output. (c) The waveform of SVD-KSES. (d) The envelope spectrum of SVD-KSES output.

## 6. Conclusion

This paper combines the signal decomposition potential of SVD and the outstanding performance of TEO to extract fault feature of a defective bearing from the vibration signal. Considering the more informative SC selection and fault delivery potential, kurtosis of TEO spectrum is proposed as a criterion to pick out the SC which has a relatively higher capacity to extract defective signature. Then, the bearing fault can be recognized from the TEO spectrums of the output of SVD-AKTEO. Moreover, the proposed SVD-AKTEO also evaluates the influence of each single SC to the accumulative SC, which is conducted in an iteration algorithm that each SC is added to the ASC one by one. The numerical simulation validates the efficiency of SVD-AKTEO with a signal buried in a heavy noise environment where the SNR reaches −13 dB and the contrastive analysis with our previous works. Moreover, a run-to-failure experiment in which the bearing performance deteriorates naturally from normal operation to its failure is considered here for experimental validation, which is very close to real industrial application. The comparative experimental results verify the effectiveness to detect the bearing outer raceway defect at an early time point. Finally, the experimental data analysis validates the capacity of SVD-AKTEO in bearing fault diagnosis. From the present work, it can be found that the singular order affects the signal decomposition performance of SVD-based methods, which lays our future research work.

## Abbreviations

REB: Rolling element bearing
TEO: Teager energy operator
KTEO: Kurtosis of Teager energy operator
SVD: Singular value decomposition
SC: Singular component
SV: Singular value
SVR: Singular value ratio
VMD: Variational mode decomposition
ASC: Accumulative singular component
ACK: Accumulative component kurtosis
SES: Squared envelope spectrum

CNN: Convolutional neural networks
FCF: Fault characteristic frequency.

## Data Availability

All experiment data used during this research are openly available from the IMS Bearing Data deposited in https://doi.org/10.1016/j.jsv.2005.03.007. Specifically, the experiment data in our manuscript are downloaded from the IMS Bearing Data, which were generated by the NSF I/UCR Center for Intelligent Maintenance System with support from Rexnord Corp. in Milwaukee, WI. In addition, the experiment data include three datasets, and the second one is employed in our manuscript to verify our proposed method (the experimental data is available online, https://ti.arc.nasa.gov/tech/dash/groups/pcoe/prognostic-data-repository/).

## Conflicts of Interest

The authors declare that they have no conflicts of interest.

## Acknowledgments

This work was supported by the National Natural Science Foundation of China (grant no. 51175419), the National Key R&D Program of China (grant no. 2018YFB2000505), and the Shaanxi Key Laboratory of Machinery Manufacturing Equipment Construction Project. Moreover, the authors are grateful to the Center of Intelligence Maintenance System (IMS), University of Cincinnati for freely providing the experimental data.

## References

[1] Y. Li, X. Liang, and M. J. Zuo, "Diagonal slice spectrum assisted optimal scale morphological filter for rolling element bearing fault diagnosis," *Mechanical Systems and Signal Processing*, vol. 85, pp. 146–161, 2017.

[2] H. Shao, H. Jiang, F. Wang, and H. Zhao, "An enhancement deep feature fusion method for rotating machinery fault diagnosis," *Knowledge-Based Systems*, vol. 119, pp. 200–220, 2017.

[3] J. Zhao, M. Sayadi, F. Fnaiech et al., "Importance of the fourth and fifth intrinsic mode functions for bearing fault diagnosis," in *Proceedings of the 14th International Conference on Sciences and Techniques of Automatic Control & Computer Engineering—STA'2013*, Sousse, Tunisia, December 2013.

[4] D. Zhang, M. Entezami, E. Stewart, C. Roberts, and Y. Dejie, "Adaptive fault feature extraction from wayside acoustic signals from train bearings," *Journal of Sound and Vibration*, vol. 425, pp. 221–238, 2018.

[5] A. Kumar and S. K. Ghosh, "Size distribution analysis of wear debris generated in HEMM engine oil for reliability assessment: a statistical approach," *Measurement*, vol. 131, pp. 412–418, 2019.

[6] Y. Cekic and L. Eren, "Broken rotor bar detection via four-band wavelet packet decomposition of motor current," *Electrical Engineering*, vol. 100, no. 3, pp. 1957–1962, 2017.

[7] H. Saruhan, S. Sandemir, A. Ç nde, and I. Uygur, "Vibration analysis of rolling element bearings defects," *Journal of Applied Research and Technology*, vol. 12, no. 3, pp. 384–395, 2014.

[8] A. Uygur and S. H. Upadhyay, "A review on signal processing techniques utilized in the fault diagnosis of rolling element bearings," *Tribology International*, vol. 96, pp. 289–306, 2016.

[9] Z. Huo, Y. Zhang, L. Shu, and M. Gallimore, "A new bearing fault diagnosis method based on fine-to-coarse multiscale permutation entropy, laplacian score and SVM," *IEEE Access*, vol. 7, pp. 17050–17066, 2019.

[10] A. Chen and T. R. Kurfess, "Signal processing techniques for rolling element bearing spall size estimation," *Mechanical Systems and Signal Processing*, vol. 117, pp. 16–32, 2019.

[11] F. Cong, J. Chen, G. Dong, and F. Zhao, "Short-time matrix series based singular value decomposition for rolling bearing fault diagnosis," *Mechanical Systems and Signal Processing*, vol. 34, no. 1-2, pp. 218–230, 2013.

[12] X. Zhao and B. Ye, "Selection of effective singular values using difference spectrum and its application to fault diagnosis of headstock," *Mechanical Systems and Signal Processing*, vol. 25, no. 5, pp. 1617–1631, 2011.

[13] X. L. Wang, Y. X. Zhang, J. P. Zhu, and Z. Q. Shi, "Research on rolling element bearing fault diagnosis based on singular value decomposition and kurtosis criterion," *Applied Mechanics and Materials*, vol. 432, pp. 304–309, 2013.

[14] M. Shi and X. Jia, "A novel strategy for signal denoising using reweighted SVD and its applications to weak fault feature enhancement of rotating machinery," *Mechanical Systems and Signal Processing*, vol. 94, pp. 129–147, 2017.

[15] L. Li, Y. Cui, R. Chen, X. Liu, and Y. Cao, "Incipient fault diagnosis of rolling bearing using accumulative component kurtosis in SVD process," *Journal of Vibroengineering*, vol. 20, no. 3, pp. 1443–1458, 2018.

[16] L. Li, Y. Cui, R. Chen, and X. Liu, "Optimal SES selection based on SVD and its application to incipient bearing fault diagnosis," *Shock and Vibration*, vol. 2018, Article ID 8067416, 13 pages, 2018.

[17] H. Zhao and L. Li, "Fault diagnosis of wind turbine bearing based on variational mode decomposition and Teager energy operator," *IET Renewable Power Generation*, vol. 11, no. 4, pp. 453–460, 2017.

[18] K. Zheng, T. Li, B. Zhang, Y. Zhang, J. Luo, and X. Zhou, "Incipient fault feature extraction of rolling bearings using autocorrelation function impulse harmonic to noise ratio index based SVD and teager energy operator," *Applied Sciences*, vol. 7, no. 11, 2017.

[19] X. Xu, M. Zhao, J. Lin, and Y. Lei, "Envelope harmonic-to-noise ratio for periodic impulses detection and its application to bearing diagnosis," *Measurement*, vol. 91, pp. 385–397, 2016.

[20] T. Barszcz and A. JabŁoński, "A novel method for the optimal band selection for vibration signal demodulation and comparison with the Kurtogram," *Mechanical Systems and Signal Processing*, vol. 25, no. 1, pp. 431–451, 2011.

[21] Y. Miao, M. Zhao, and J. Lin, "Periodicity-impulsiveness spectrum based on singular value negentropy and its application for identification of optimal frequency band," *IEEE Transactions on Industrial Electronics*, vol. 66, no. 4, pp. 3127–3138, 2019.

[22] S. Lin, G. Tang, X. Wang, and Y. He, "Time-frequency analysis based on improved variational mode decomposition and teager energy operator for rotor system fault diagnosis," *Mathematical Problems in Engineering*, vol. 2016, Article ID 1713046, 9 pages, 2016.

[23] J. Ma, J. Wu, and X. Wang, "Incipient fault feature extraction of rolling bearings based on the MVMD and Teager energy operator," *ISA Transactions*, vol. 80, pp. 297–311, 2018.

[24] M. Wang, Z. Jiang, and K. Feng, "Research on variational mode decomposition in rolling bearings fault diagnosis of the multistage centrifugal pump," *Mechanical Systems and Signal Processing*, vol. 93, pp. 460–493, 2017.

[25] H. Qiu, J. Lee, J. Lin, and G. Yu, "Wavelet filter-based weak signature detection method and its application on rolling element bearing prognostics," *Journal of Sound and Vibration*, vol. 289, no. 4-5, pp. 1066–1090, 2006.

[26] Y. Lv, R. Yuan, T. Wang, H. Li, and G. Song, "Health degradation monitoring and early fault diagnosis of a rolling bearing based on CEEMDAN and improved MMSE," *Materials*, vol. 11, no. 6, 2018.

[27] D. Abboud, M. Elbadaoui, W. A. Smith, and R. B. Randall, "Advanced bearing diagnostics: a comparative study of two powerful approaches," *Mechanical Systems and Signal Processing*, vol. 114, pp. 604–627, 2019.